ChemComm

Cite this: *Chem. Commun.*, 2011, **47**, 8349–8351

www.rsc.org/chemcomm

COMMUNICATION

Ester hydrogenation catalyzed by Ru-CNN pincer complexes†

Yunshan Sun, Christian Koehler, Runyu Tan, Vincent T. Annibale and Datong Song*

Received 3rd May 2011, Accepted 5th June 2011
DOI: 10.1039/c1cc12601f

We report new Ru-CNN pincer catalysts for ester hydrogenation under mild conditions.

The reduction of esters to the corresponding alcohols is an important chemical process that has found use in many areas. In the total synthesis of natural products and drug candidates, esters are usually reduced with a stoichiometric amount of aluminum-hydride reagent (*e.g.* $LiAlH_4$ and $AlBu_2H$),[1] which requires tedious work-up procedures to handle the resulting inorganic wastes. The catalytic hydrogenation of esters is an attractive alternative, because it produces no byproduct. In manufacturing industry, fatty esters are reduced to fatty alcohols in the presence of heterogeneous catalysts at 200–300 °C under 200–300 bar of H_2 gas.[2] The energy consumption and safety issues associated with these processes call for the development of better catalysts that can operate at a lower temperature under a lower pressure of H_2.

Recently, Firmenich has reported homogeneous catalysts for ester hydrogenation that operate at 100 °C with low catalyst loadings, but require the use of high pressures of H_2 (*e.g.*, 50 bar in most cases).[3] Milstein and coworkers have reported a Ru-pincer catalyst (Scheme 1a) for ester hydrogenation that operates under a much lower pressure (5.3 bar) of H_2 and at 115 °C.[4] Milstein's catalyst is effective for several esters, but the turn-over frequency (TOF) is generally low. For the bulky *tert*-butyl acetate, in particular, 10.5% yield has been observed after 24 h; the corresponding TOF is 0.44 h^{-1}. Herein, we report new Ru-CNN pincer complexes that catalyze ester hydrogenation under milder conditions (105 °C and 5.3 bar) with a significantly higher performance than Milstein's catalyst. For example, the catalytic hydrogenation of *tert*-butyl acetate with our catalytic system shows a more than 100-fold increase in TOF at a lower temperature, compared to Milstein's catalytic system.

The new pyridine-based CNN pincer ligand precursors with NHC and diethylamino arms can be synthesized from 2,6-bis(bromomethyl)pyridine *via* two successive nucleophilic substitutions with appropriate imidazoles and diethylamine in good yields (see ESI†). Complexation can be achieved by reacting $[RuHCl(CO)(PPh_3)_3]$ with free carbenes **1a** and **1b** (Scheme 1) that are generated *in situ* from the corresponding imidazolium ligand precursors and LiHMDS (HMDS = bis(trimethylsilyl)amide). The resulting Ru-CNN pincer complexes are mixtures of [RuH(CNN)(CO)Br] (major ~98%) and [RuH(CNN)(CO)Cl] (minor ~2%), which can be converted into pure [RuH(CNN)(CO)Br], **2a** and **2b** by reacting with LiBr.[5]

Complexes **2a** and **2b** are air stable in the solid state. They are slightly soluble in benzene and slowly react with chloroform. Because **2a** and **2b** show similar properties, we will use **2a** as an example for further discussions. In the ^1H NMR spectrum of **2a** in C_6D_6, the four pyridylic protons display 4 doublets at 6.97 and 4.20 ppm (NHC-CH_2Py), 3.79 and 3.36 ppm (PyCH_2NEt_2). The hydride ligand exhibits a singlet at −14.21 ppm. The structures of **2a** and **2b** have been unambiguously confirmed with X-ray crystallography (Fig. 1). The pincer ligand adopts a *mer* configuration. Each Ru(II) center adopts a distorted octahedral coordination geometry with a CO ligand *trans* to a pyridine nitrogen atom, and a hydride *trans* to a bromide. The six-membered chelate ring involving the NHC donor adopts a boat conformation, with the axial pyridylic proton aligned with the bromide ligand. The axial pyridylic proton of the amine arm is aligned with the hydride ligand. The Ru1–N1 bond (2.256(2) and 2.262(2) Å for **2a** and **2b**, respectively) is significantly longer than Ru1–N2 bond (2.134(2) and 2.135(2) Å for **2a** and **2b**, respectively) as a result of the strong *trans*-influence of the carbene donor.

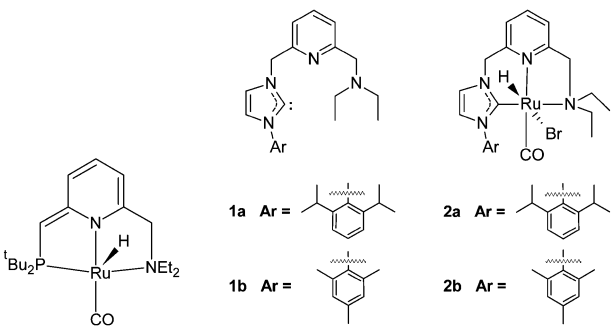

Scheme 1 (a) Milstein's catalyst; (b) NHC-based CNN-pincer ligands **1a**, **1b** and the corresponding Ru(II) complexes **2a**, **2b**.

Davenport Chemical Research Laboratories, Department of Chemistry, University of Toronto, 80 St. George Street, Toronto, Ontario, Canada. E-mail: dsong@chem.utoronto.ca; Fax: +1-416-978-7013; Tel: +1-416-978-7014

† Electronic supplementary information (ESI) available: Experimental procedures and characterization details. CCDC 824073–824077. For ESI and crystallographic data in CIF or other electronic format see DOI: 10.1039/c1cc12601f

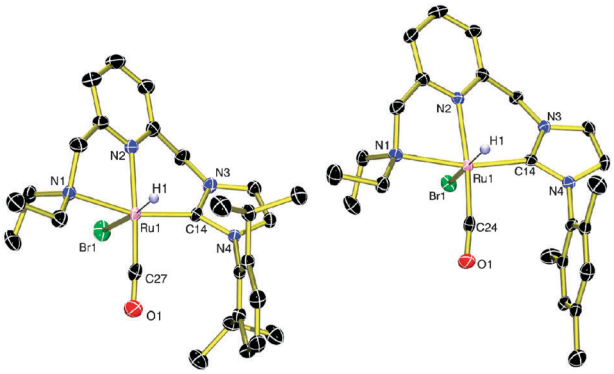

Fig. 1 Pov-Ray plots of the molecular structures of complexes **2a** (left) and **2b** (right) with thermal ellipsoids plotted at 50%. All H atoms are omitted for clarity except for hydrides.

In the presence of KO^{t}Bu or KHMDS, **2a** catalyzes the H_2-hydrogenation of esters with high efficiencies at 105 °C, under 5.3 bar of H_2. As shown in Table 1, a variety of unactivated aliphatic and aromatic esters can be hydrogenated into the corresponding alcohols in excellent to quantitative yields within 2 or 3 h (entries 1–7). The simple ethyl acetate can be hydrogenated in quantitative yield within 2 h (entry 4), while with Milstein's catalyst, 86% yield takes 12 h to achieve. Remarkably, even the bulky ester *tert*-butyl acetate can be hydrogenated in 93% yield within 2 h (entry 6), while Milstein's catalyst gives 10.5% yield in 24 h. A diester diethyl succinate can be hydrogenated into the corresponding diol in quantitative yield within 2 h (entry 7). Complexes **3a** and **4a** can also catalyze the hydrogenation of esters under similar conditions as shown above with similar efficiencies. The activities of **2b** and its derivatives are slightly lower.

To probe the mechanism of the catalytic cycle, we conducted stoichiometric reactivity studies. When **2a** is reacted with 1 equiv of KHMDS in solution (Scheme 2), the clean formation of **3a** can be observed *via* NMR experiments. In the ^{1}H NMR spectrum of **3a** in C_6D_6, the hydride ligand displays a singlet at −22.69 ppm. The two doublets from the pyridylic protons of the NHC arm of **2a** are replaced by a singlet integrated as 1 proton at 6.13 ppm; the corresponding carbon resonates at 95.6 ppm in the ^{13}C NMR spectrum. The pyridine proton *para* to the NHC arm shows a significant upfield shift upon deprotonation: from 6.37 ppm in **2a** to 5.48 ppm in **3a**, indicating the dearomatization of the pyridine ring. The other two protons of the pyridine ring show smaller upfield shifts. The two pyridylic protons of the amine arm remain inequivalent, displaying two doublets at 3.38 and 2.71 ppm, respectively. No deprotonation at the amine arm was observed. Our DFT calculations show that the observed deprotonation product **3a** is 9.5 kcal mol^{-1} more stable than its isomer with a deprotonated amine arm in terms of free energy, consistent with the observation that **3a** is the only observable product of deprotonation (see ESI† for details). Under similar conditions, the deprotonation of **2b** does not proceed cleanly. Presumably, the labile amine-arm of the pincer ligand may dissociate from the metal center and the less bulky mesityl group of the ligand may allow for aggregation of the resulting 5-coordinate complex. However, when 1 equiv. of PPh_3 is added to the reaction mixture (Scheme 3), everything cleanly converts to one species, **3b**, whose structure has been confirmed with X-ray crystallography (Fig. 2). The C–C bond lengths of the C_5N ring shows the alternating short-long pattern, *i.e.*, C6–C7 1.363(7), C7–C8 1.419(7), C8–C9 1.360(7), C9–C10 1.445(7) Å. The C10–C11 bond length is 1.367(7) Å, consistent with a typical double bond. It is clear that the NHC arm is deprotonated and the pyridine ring is dearomatized. The addition of PPh_3 has trapped the 5-coordinate species as a monomeric 6-coordinate adduct.

Next, we studied the reactivity of **3a** towards dihydrogen. Under ~3.8 atm of H_2 at room temperature **3a** can be converted into **4a** (Scheme 2). The ^{1}H NMR spectrum of **4a** in C_6D_6 shows only one singlet in the hydride region at −4.35 ppm, indicative for a *trans*-dihydride species.[6] A singlet (2H, NHC-CH_2Py) at 4.66 ppm and a singlet (2H, PyCH_2NEt$_2$) at 3.81 ppm can be attributed to the two methylene linker groups, respectively. The resonances at 6.74, 6.41, and 6.33 ppm can be attributed to the protons of the rearomatized pyridine ring. Under an N_2 atmosphere at room temperature **4a** slowly loses H_2 in solution to regenerate **3a**; Milstein's Ru-PNN *trans*-dihydride species displays a similar behavior.[6] To gain further insight into the H_2 activation process (*e.g.*, the fate of each H atom in H_2), we studied the reaction between **3a** and D_2. At −78 °C a toluene solution of **3a** reacts with 1 atm of D_2 to afford instantaneously **4a**-d_2 (Scheme 4), in which deuterium atoms are incorporated into the pyridylic position of the NHC arm and on the metal center, as confirmed by ^{1}H and ^{2}H NMR experiments. Interestingly, when the reaction mixture is warmed to room temperature the pyridylic position of the amine arm also gets deuterated. At room temperature overnight, all four pyridylic protons and the two hydrides become deuterated, affording **4a**-d_6. This indicates that the hydrogen splitting and releasing processes are dynamic and that the dearomatization–rearomatization process also involves the amine arm. No parallel reactivity (*i.e.*, the involvement of both arms) was reported for Milstein's PNN system. Interestingly, X-ray crystallography shows that **4a** exists as a dimer in the solid state (Fig. 2S in ESI†), with two bridging hydrides and dangling amine arms, indicating the labile nature of the amine arm.

Using acetophenone as the model substrate, we studied the hydrogenation in a stepwise manner (Scheme 5). When *trans*-dihydride **4a** is treated with 1.05 equiv. of acetophenone in C_6D_6 at ambient temperature under N_2 a dynamic reaction mixture is achieved, as evidenced by the broad signals in the ^{1}H NMR spectrum. Alternatively, the same reaction mixture can be achieved by reacting **3a** with 1 equiv. of 1-phenylethanol at ambient temperature. At 60 °C, the ^{1}H NMR spectrum of the reaction mixture becomes cleaner (*i.e.*, with one dominant species, **5a**) and the signals are sharper. The appearance of the characteristic signal at 5.47 ppm indicates a dearomatized ligand backbone; no free 1-phenylethanol is present. Therefore, the quartet and doublet at 4.62 and 1.32 ppm, respectively, are tentatively assigned to a coordinating 1-phenylethanol in **5a**. Under ~4.3 atm of H_2 at 60 °C **5a** converts into **4a** and 1-phenylethanol cleanly within minutes. In this process, **3a** could not be observed, presumably because of the fast conversion of **3a** to **4a** under H_2. Further experiments and DFT calculations will be carried out to help elucidate the

Table 1 Hydrogenation of esters to alcohols catalyzed by complex **2a** in the presence of KO^{t}Bu[a]

Entry	Substrate	t (h)	Conv. (%)[b]	Yield (%)[d]
1[c]	PhCOOEt	2	99.6	$PhCH_2OH$ (97.7) EtOH (99)
2	$PhCH_2COOEt$	2	99.7	$PhCH_2CH_2OH$ (99.7) EtOH (98)
3	CH_3COOCH_3	2	96	EtOH (96) MeOH (96)
4	CH_3COOEt	2	99	EtOH (99)
5	CH_3COOCH_2Ph	3	90	$PhCH_2OH$ (90) EtOH (87)
6	$CH_3COOCMe_3$	2	93	EtOH (93) ^{t}BuOH (92)
7[e]	$(CH_2COOEt)_2$	2	99	$HO(CH_2)_4OH$ (99) EtOH (99)

[a] Ester (1 mmol), complex **2a** (0.01 mmol), KO^{t}Bu (0.08 mmol) and toluene (2 mL), 105 °C, 5.3 bar of H_2. [b] Conversions were determined by GC with mesitylene as the internal standard. [c] 0.01mmol of KO^{t}Bu was used. [d] Yields were determined by ^{1}H NMR with mesitylene as the internal standard. [e] 0.02 mmol of **2a** was used.

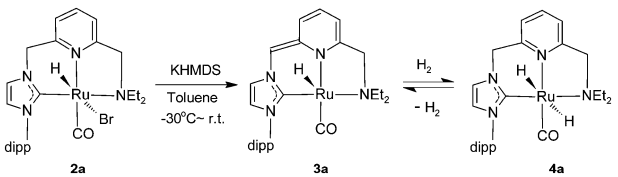

Scheme 2 Syntheses of **3a** and **4a**.

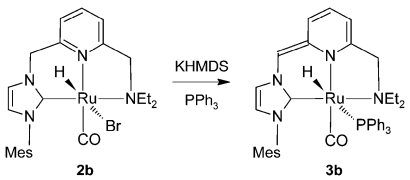

Scheme 3 Synthesis of **3b**.

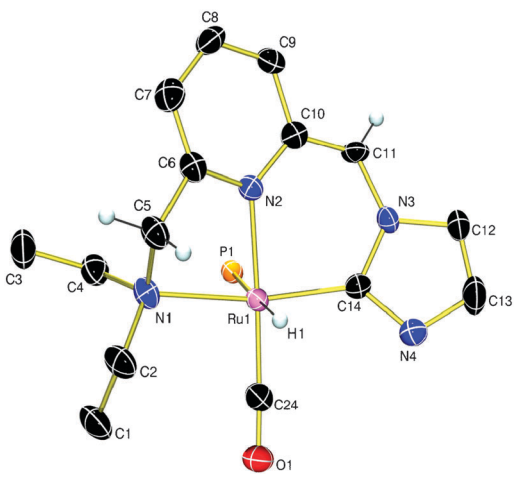

Fig. 2 Pov-Ray plot of the molecular structure of **3b** with thermal ellipsoids plotted at 50%. All H atoms are omitted for clarity except for hydrides and pyridilic protons. The phenyl groups of PPh_3 and the mesityl group of the NHC arm are omitted for clarity.

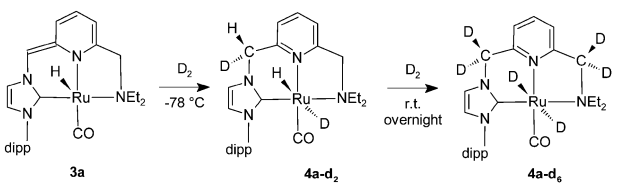

Scheme 4 Deuterium scrambling experiments.

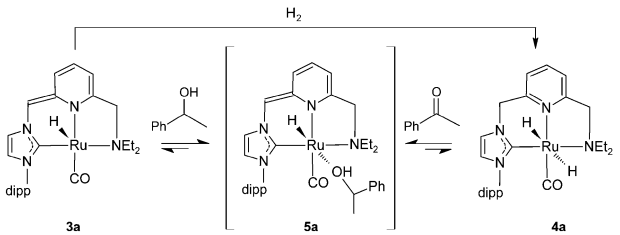

Scheme 5 Stepwise hydrogenation study.

energetics of different species in the reaction system as well as the mechanism of the catalytic reaction.

In summary, we have synthesized and characterized two new NHC-based CNN-pincer ligands and the corresponding ruthenium (II) complexes **2**. Complex **2a** can be deprotonated by a strong base to form a 5-coordinate species **3a** with dearomatized pyridine moiety in the ligand backbone. Compound **3a** can split H_2 to form a *trans*-dihydride species **4a** with a rearomatized pyridine moiety in the ligand backbone. Interestingly, the D_2 experiment reveals that both pincer arms participate in the H_2 activation and releasing processes. Complexes **2** in the presence of KO^{t}Bu or KHMDS catalyze the H_2-hydrogenation of unactivated esters under mild conditions. Even the bulky ester *tert*-butyl acetate, which cannot be effectively hydrogenated by the Ru-PNN system, can be converted into the corresponding alcohols in excellent yield. Our work represents a rare example of a phosphorus-free pincer system that displays the dearomatization–rearomatization type of metal–ligand cooperation. The detailed mechanism and the scope of polar bond hydrogenation as well as other reactivities of this new Ru-CNN system are being investigated in our laboratory.

Notes and references

1 S. N. Ege, *Organic Chemistry*, D. C. Heath and Company, Lexington, 1989, p. 596.
2 Y. Pouilloux, F. Autin and J. Barrault, *Catal. Today*, 2000, **63**, 87, and references therein.
3 L. A. Saudan, C. M. Saudan, C. Debieux and P. Wyss, *Angew. Chem. Int. Ed.*, 2007, **46**, 7473–7476.
4 J. Zhang, G. Leitus, Y. Ben-David and D. Milstein, *Angew. Chem., Int. Ed.*, 2006, **45**, 1113–1115.
5 The mixture of [RuH(CNN)(CO)Br] and [RuH(CNN)(CO)Cl] can be used for reactivity studies directly, because the deprotonation of both species gives the same 5-coordinate species. For details, see ESI†.
6 J. Zhang, G. Leitus, Y. Ben-David and D. Milstein, *J. Am. Chem. Soc.*, 2005, **127**, 10840–10841.